

Pharmaceutical Interactions of Verapamil Hydrochloride and Citric Acid: An In Vitro Analysis

Abstract

The objective of this study is to investigate the combination of drug-drug interactions involving different functional groups by assessing the interaction of a BCS class IV compound (Verapamil HCl) with Citric acid in various ratios, thereby enhancing the understanding of pharmacological implications. This study elucidated the compatibility between Verapamil HCl and Citric acid, demonstrating an approach to enhance the solubility, permeability, and bioavailability of poorly water-soluble drugs in pharmaceutical applications.

The method of solvent evaporation was utilized for the preparation of solid dispersions. This process involved dissolving the active pharmaceutical ingredient and citric acid in ethanol, evaporating the solvent to yield a solvent-free film, and mechanically reducing the residue using a mortar and pestle. The resultant fine powder was sieved through a 40-mesh filter and appropriately stored in vials for subsequent analyses.

FT-IR spectra and an HPLC-sensitive method were employed to evaluate the solubility profile and interaction dynamics of the compound. FT-IR spectra of VPM HCl and its physical mixtures with citric acid at ratios of 1:3, 1:5, and 1:7 were obtained using an FT-IR spectrophotometer. The spectra revealed structural and functional group alterations, quantified by analyzing the magnitude and cumulative area of the peaks corresponding to the structural constituents.

In accordance with the established linearity, the retention times for VPM HCl, Sample 1, Sample 2, and Sample 3 were recorded as 6.8 ± 0.2 , 2.7 ± 0.1 , 5.5 ± 0.2 , and 3.8 ± 0.1 minutes, respectively, across a concentration range of 1–100 $\mu\text{g/mL}$. For all analytes, the intra-assay and inter-assay biases were observed to be within 15% and 13.4%, respectively. Furthermore, in vitro evaluations of physical combinations of PNT and VTB samples revealed minimal interaction.

These findings emphasize the stability and compatibility of Verapamil HCl and citric acid, demonstrating citric acid's role as a reliable excipient for enhancing drug solubility and bioavailability without compromising therapeutic integrity.

Comment [AS1]: •Briefly explain, rationale for the use of solvent evaporation.
• Ensure the Pharmaceutical technical terminology to understanding for all readers.

1. INTRODUCTION

In pharmaceutical science and clinical practice, drug interactions are a major problem that significantly impacts the pharmacokinetics, safety, and effectiveness of therapeutic drugs (Bialer et al., 2012; Wen et al., 2015). Among them, the interaction between excipients and active pharmaceutical ingredients (APIs) demands particular attention. The reason is - even if excipients are regarded as inert historically, they still greatly

affect API stability and bioavailability (Gorain et al., 2018). Renowned pH-modifying excipient citric acid, for example, can change the chemical environment of the API, thus affecting its solubility, stability, absorption, and other pharmacokinetic characteristics (Lambros et al., 2022). These interactions are therefore quite important to analyse since they can affect compliance with regulatory criteria and treatment results.

Verapamil hydrochloride (Verapamil HCl) is a widely prescribed medication for patients diagnosed with cardiovascular diseases like hypertension, angina, arrhythmias, etc. owing to its unique mechanism as a calcium channel blocker (Zhou et al., 2013; Nadimi et al., 2018; Cinar et al., 2024). Its therapeutic performance relies on its molecular stability (Bezzon, et al., 2021). However, with the presence of reactive excipients like citric acid, its performance can be compromised (Li et al., 2019). Hence, the stability and integrity of Verapamil HCl might be affected because of citric acid. Despite its clinical importance, the mechanism of Verapamil HCl-citric acid at a chemical level is still largely unexplored, revealing a substantial gap in the existing research. The paper will examine the interaction dynamics, emphasising their relevance in pharmaceutical development and clinical practice.

Citric acid is an excipient that is used in many drug formulations. It helps to adjust pH levels in the drugs, and it helps to make the drugs more soluble (Ghorpade et al., 2017; Nangare et al., 2021). However, citric acid might react with APIs that are a little unstable which can lead to degradation of the API or to the formation of new, unexpected, and possibly dangerous compounds (Fung, et al., 2018). This raises the question of whether citric acid remains a "benign" additive in these contexts. Investigating these interactions is essential since formulations with intrinsically unstable APIs must make sure that excipients do not affect the stability of the active ingredients anymore (Govindarajan et al., 2015).

The primary objective of this study is to determine the nature of the interaction between Verapamil HCl and Citric acid. In other words, this study seeks to determine whether their interaction is purely physical—that is, whether just solubility changes or also involves chemical changes, such as degradation of the API or synthesis of a new compound. This work also investigates if there is any molecular alterations due to the interaction between Verapamil HCl and Citric acid and also evaluates the drug performance.

To achieve these objectives, a multi-analytical approach was employed. We performed high-performance liquid chromatography (HPLC), Fourier-transform infrared (FTIR) spectroscopy, and ultraviolet-visible (UV-Vis) spectroscopy tests to determine the type of interaction. HPLC facilitated the precise separation and quantification of reaction products (Shomudro et al., 2022; Yin et al., 2023). It helps to evaluate Verapamil HCl's stability in the presence of citric acid. FTIR spectroscopy provided molecular insights into functional group alterations, revealing chemical bond changes associated with the interaction (Faghihzadeh et al., 2016). And lastly, we used UV-Vis spectroscopy to detect electronic transitions that signify structural modifications to Verapamil HCl (Shinkar et al., 2018).

The experimental conditions were carefully controlled to mimic pharmaceutical and physiological environments. These settings included different concentrations and pH levels in order to simulate situations that could occur in formulations or in the gastrointestinal tract. This systematic approach allowed for a comprehensive investigation of interaction dynamics, highlighting specific conditions that may compromise Verapamil HCl's stability.

The results of this investigation have substantial implications for clinical practice and pharmaceutical research. This study questions the presumption of excipient inertness by characterising the interaction between Verapamil HCl and citric acid, thus providing an enhanced understanding of API-excipient interactions. These discoveries can direct towards the development of more stable and reliable drug formulations. Furthermore, the research emphasises the need for sophisticated analytical methods to understand the complexity of drug-excipient interactions and provides a strong basis for further research.

2. MATERIALS and METHOD

2.1 Materials

The drug Verapamil HCl and the carrier Citric acid was obtained from Incepta Pharmaceutical Ltd. Bangladesh. Ethanol was used for experimental purpose which was of analytical grade and was collected from laboratory of Stamford University Bangladesh.

2.2 *In Vitro* Drug–Drug Interaction Study

2.2.1 Sample Preparation

The solvent evaporation technique was employed for the preparation of solid dispersions. The ideal conditions for synthesizing Verapamil HCl (VPM HCl) involved precise measurement of the carrier, Citric acid, using a digital balance at various ratios (1:3, 1:5, 1:7). This physical mixture was then solubilized in an appropriate volume of ethanol within a 250 mL Round Bottom Flask (RBF) until complete dissolution was achieved. The solvent was subsequently evaporated utilizing a water bath equipped with a digital temperature controller, maintaining a temperature of 60°C until a wet mass was achieved. The residue was collected and subsequently placed in a hot air oven for drying until a constant weight was attained.

2.2.2 Fourier Transform Infrared Spectroscopy (FT-IR)

FTIR analyses were performed using a FTIR spectrometer). Data were collected over a spectral region from 4000 to 400 cm^{-1} with a resolution of 4 cm^{-1} . The FT-IR analysis indicated the potential for hydrophobic interactions occurring between citric acid and VPM HCl. The samples were individually positioned on the sample platform of the instrument (Perkin Elmer, L160000A, Waltham, MA, USA), and infrared spectra were

acquired within the range of 4000–600 cm^{-1} utilizing Spectrum 10 STD software (Srinivasan et al., 2011). Throughout the analysis, the baseline underwent correction and normalization for each individual sample.

2.3 Method Development

2.3.1. Instrumentation

The Shimadzu HPLC system (LC-20A VP, Shimadzu, Kyoto, Japan) with UV detection was used to determine the content of PNT, VTB1, VTB6, and VTB12. It included an SPD-20Avp UV-vis detector, a CTO-20Avp column oven, an LC-20ADvp solvent delivery pump, a DGU-14A degasser, and a SCL-10Avp system controller. With an ODS, reversed-phase C18, 150 mm \times 4.6 mm, 5 μm column kept at 35 $^{\circ}\text{C}$, the analysis was carried out at 280 nm wavelength.

2.3.2 Preparation of Stock and Working Standard Solutions

The internal standard (IS) (VPM HCl at a fixed concentration of 10 $\mu\text{g}/\text{mL}$), Sample 1 (100 $\mu\text{g}/\text{mL}$), Sample 2 (100 $\mu\text{g}/\text{mL}$), and Sample 3 (100 $\mu\text{g}/\text{mL}$) were all individually produced in methanol and kept out of direct sunlight at -20 $^{\circ}\text{C}$. The stock solutions were serially diluted with methanol to create the working solutions (Studzińska-Sroka et al., 2018).

2.3.3 Chromatographic Separation

Using HPLC-grade water A and acetonitrile as mobile phase B in linear gradient elution mode (A:B), PNT, VTB1, VTB6, and VTB12 were separated on a Phenomenex C18 column (150 \times 4.6 mm) with a 5 μm particle size (UV detector 20A, Shimadzu, Kyoto, Japan). The following were the mobile phase's gradient conditions: 0–20 minutes. The column temperature was maintained at 35 $^{\circ}\text{C}$, and the flow rate was fixed at 0.5 mL/min. An internal standard technique was employed to examine the filtrate using a Shimadzu HPLC system, as detailed in the previous section. At a wavelength of 280 nm, the Standard, Sample 1, Sample 2, and Sample 3 were all analyzed concurrently (Sanam et al., 2023).

2.4. Method Validation

The following factors were assessed in order to verify the HPLC method: recovery, accuracy, precision, sensitivity, specificity, and selectivity. Sensitivity was assessed using limits of detection (LOD) and limits of quantitation (LOQ), which are concentrations with a signal-to-noise ratio of at least 3 and 10, respectively (Alquadeib et al., 2019). A least-squares regression line was computed in order to evaluate the correlation coefficient (r), which stands for linearity. As previously stated, the intra- and inter-day precision and accuracy were assessed using three quality control (QC) samples at low, medium, and high concentrations of 10, 20, and 30 ($\mu\text{g}/\text{mL}$, respectively). Intra-day precision was determined by calculating the recovery percentage for the QC samples in triplicate. The inter-day accuracy was estimated by analyzing the QC samples on three separate days. The accuracy of an analytical

Comment [AS2]: Please briefly explain why the internal standard (IS) was included (e.g., for normalization, quantification, or calibration).

Comment [AS3]: Please explain the homogeneity of Stock Solutions before storage.

Comment [AS4]: •The gradient conditions are partially mentioned as "0–20 minutes" without specifying the exact proportions of mobile phases A and B at each stage of the gradient. This information is crucial for reproducibility.
•Must be explain on how the samples (Standard, Sample 1, Sample 2, and Sample 3) were prepared or processed before injection, including filtration or dilution steps.

procedure is expressed by how closely the value found matches the predicted value. It is measured by calculating the analyte's recovery percentage (%R). In this case, the accuracy of the process was evaluated by doing three follow-up analyses ($n = 3$) using the recommended method for three different concentrations of standard sample solution (10 $\mu\text{g/mL}$, 20 $\mu\text{g/mL}$, and 30 $\mu\text{g/mL}$) (Bulduket al., 2021). The experiment's outcomes were statistically examined using the formula [%Recovery = (Recovered conc./Injected conc.) \times 100] in order to assess the recovery and validity of the suggested approach. Target analyte stability in plasma was assessed for up to 24 hours at 4 °C and room temperature, for up to two weeks at -80 °C, and during three freeze-thaw cycles (Sahu, et al., 2018).

2.5 Statistical Analysis

The mean \pm standard deviation (SD) is used to represent all data. The graphs were made using GraphPad, Prism 8.0 (GraphPad Software, La Jolla, CA, USA). For statistical comparisons, a one-way analysis of variance with pairwise comparisons using Fisher's least significant difference method was used. In every analysis, a p-value of less than 0.05 was deemed significant.

3. RESULT and DISCUSSIONS

To evaluate the medications' solubility, FT-IR spectra were captured. The FT-IR spectrophotometer was used to show the FT-IR spectra for VPM HCl and a physical combination of the medication and the citric acid at a ratio of (1:3, 1:5, and 1:7). The range of the scan was 400–4000 cm^{-1} . For every measurement, VPM and drug-drug (1:3, 1:5, 1:7, 1:9) mixtures may be put straight into the infrared beam's path. The disk that was KBr pressed was utilized. The medication and potassium bromide combination were weighed at a 1:1 ratio. In order to create a semi-transparent pellet that allows light to reach the detector, samples were combined in a mortar and then compressed for two to three minutes.

The following describes how the spectral signals shift and how the VPM HCl's dimension changes:

This research aims to identify drug-polymer mixtures with distinct functional groups. For VPM HCl, only a band close to 3500 cm^{-1} (N-H stretch.) was seen. The benzene ring is directly linked to the structure's backbone conformation, which is between 3200 and 2800 cm^{-1} , where sp (C-H stretching) and sp^2 (C-H stretching) were discovered. Additionally, the measurement of 1154.52 cm^{-1} shows that there is a C-O functional group present. Ultimately, varying ratios of drug-drug combinations resulted in distinct spectra. To gauge the changes in drug-polymer mixes, these structures of the free drug and drug-drug mixtures were examined, and the intensity of the relevant functional group was computed. The peaks' overall area and intensity were computed within the range of the drug's various structural elements. At varying doses, VPM HCl and citric acid interactions were permitted with 1:3 (Sample 01), 1:5 (Sample 02), and 1:7 (Sample 03).

3.2 Individual Data of Selective Compounds

Interpretation of VPM HCl and VPM HCl-Polymer mixtures were measured under physiological condition as in Figure. (01 to 05).

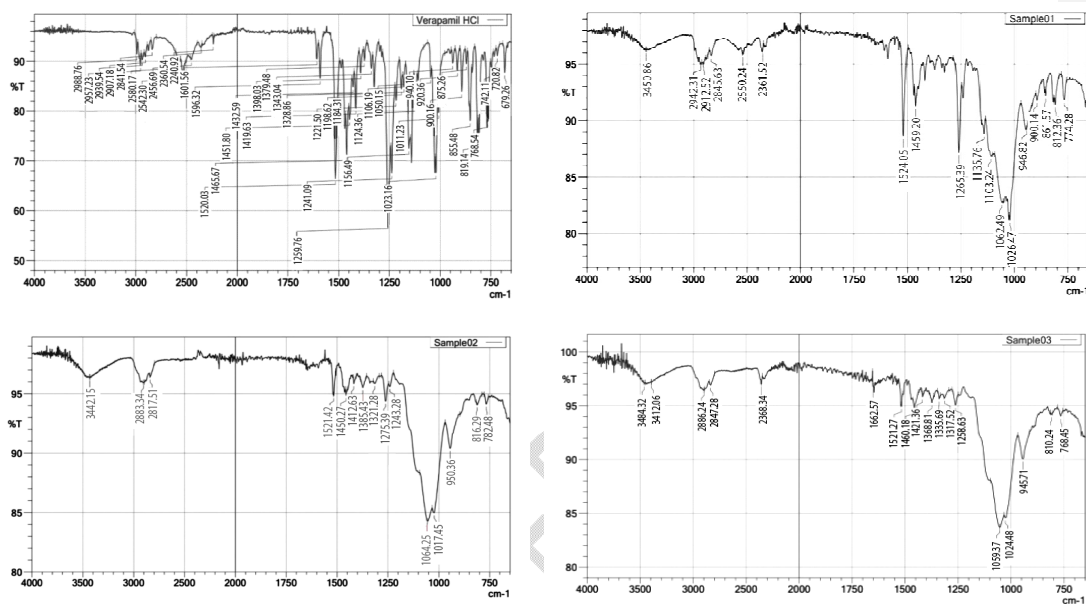


Figure 1-4: FTIR Chromatograms of Verapamil HCl and Samples 1-3. (Top-left: FTIR spectrum of Verapamil HCl; Top-right: FTIR spectrum of Sample 1; Bottom-left: FTIR spectrum of Sample 2; Bottom-right: FTIR spectrum of Sample 3).

Table 1: Some important peaks observed in FT-IR spectra of Verapamil HCl, sample 1, sample 2 and sample 3 and their composite with their possible assignment.

Peak Assignment	Peak Position (cm ⁻¹)			
	Verapamil HCl	PM of Verapamil HCl and Sample 1	PM of Verapamil HCl and Sample 2	PM of Verapamil HCl and Sample 3
N-H	3489.36	3374.09	3374.10	N/A
O-H	N/A	3137.08	3156.03	3773.21
N-H	3370.58	N/A	2944.29	3379.29
C-H	3195.28	2945.08	2845.89	2942.05
C=O	1588.56	1592.63	1590.23	1592.14
C-N	1372.59	1382.56	1382.62	1378.91
C-O	1119.94	1119.05	1117.95	N/A
S=O	1034.87	1032.21	1032.06	1034.96

Table 2: Analytical parameters for robustness of HPLC method.

Parameters	Variables	RT	Verpamil HCl % Recovery	RT	Sample 1 % Recovery	RT	Sample 2 % Recovery	RT	Sample 3 % Recovery
Flow rate (mL/min)	0.3	13.3	82.8 ± 5.28	5.2	114.30 ± 2.59	9.3	113.25 ± 2.08	6.6	67.55 ± 2.85
	0.5	6.5	124.50 ± 8.29	3.5	84.15 ± 2.75	5.6	97.85 ± 2.87	4.4	108.44 ± 1.27
Mobile Phase	Acetonitrile	7.6	124.50 ± 8.29	3.5	84.15 ± 2.75	3.5	97.85 ± 2.87	4.4	108.44 ± 1.27
	Methanol	ND	ND	ND	ND	ND	ND	ND	ND
Column (µm)	250 × 4.7	9.1	103.25 ± 3.54	3.3	78.25 ± 2.29	ND	ND	ND	ND
	150 × 4.7	6.7	124.50 ± 8.29	2.8	84.15 ± 2.75	5.6	97.85 ± 2.87	3.7	108.44 ± 1.27
Wavelength (nm)	275	ND	ND	ND	ND	ND	ND	4.1	65.77 ± 4.68
	285	7.6	124.50 ± 8.29	3.1	84.15 ± 2.75	5.6	125.54 ± 2.16	4.6	108.44 ± 1.27
	300	ND	ND	ND	ND	ND	ND	ND	ND
	500	ND	ND	ND	ND	ND	ND	4.5	126.45 ± 6.49
Column Temp (°C)	30	6.7	124.50 ± 8.29	3.3	97.85 ± 2.87	6.0	112.75 ± 4.68	4.3	108.44 ± 1.27
	35	7.6	124.50 ± 8.29	3.5	84.15 ± 2.75	5.6	97.85 ± 2.87	4.0	108.44 ± 1.27

ND and RT indicates not detected and retention time respectively; Data represent the mean ± S.D. of 3 experiments

Table 3. Analytical parameters for system suitability test of HPLC method

Parameter	Verapamil HCl	Sample 1	Sample 2	Sample 3
Retention time (min)	6.7 ± 0.3	2.8 ± 0.1	5.4 ± 0.2	3.9 ± 0.1
Assay (%)	105.08 ± 2.41	103.55 ± 2.65	115.63 ± 1.98	90.0 ± 1.58
Peak height	3540.25 ± 176.92	7310 ± 955.29	51844 ± 1750.21	3994.25 ± 632.84
No of theoretical plates	548.77 ± 71.48	1215 ± 62.03	4362 ± 1482.26	1059 ± 250.29
USP Trailing Factor	0.80 ± 0.07	1.48 ± 0.29	0.80 ± 0.3	1.82 ± 0.08
Capacity Factor	2.6 ± 1.21	0.72 ± 0.08	1.50 ± 0.50	0.80 ± 0.23
LOD (ng/mL)	0.48	0.60	15.35	0.05
LOQ (ng/mL)	1.49	1.79	69.35	0.10

Data represent the mean ± S.D. of 3 experiments

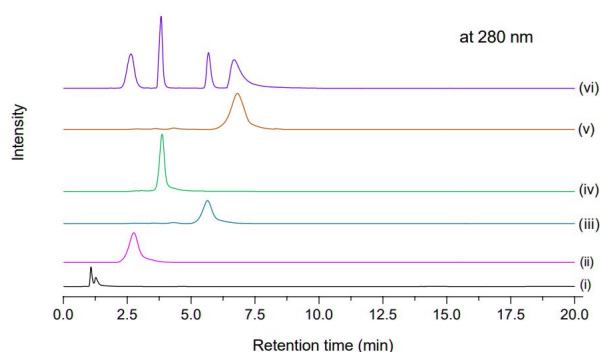


Figure 5: Standard RP-HPLC chromatograms at 280 nm. (i) Blank; (ii) Sample 1; (iii) Sample 2; (iv) Sample 3; (v) VPH

Comment [AS5]:

Table 4. Intra-day and inter-day accuracy, precision, and recovery matrix effects for Verapamil HCl, sample 1, sample 2 and sample 3 determination.

Sample	Spiked Analyte ($\mu\text{g/mL}$)	Intra Day				Inter Day			
		Mean \pm S.D	CV %	Accuracy (RE%)	Recovery (%)	Mean \pm S.D	CV%	Accuracy (RE%)	Recovery (%)
Verapamil HCl	10	14.02 \pm 0.95	7.55	- 10.76	115.10	14.05 \pm 1.48	11.27	- 11.56	114.05
	20	20.04 \pm 0.71	3.63	3.78	97.86	18.05 \pm 3.15	13.42	10.51	89.54
	30	28.34 \pm 1.35	5.28	8.64	92.05	29.64 \pm 1.02	3.51	5.47	95.10
Sample 1	10	11.87 \pm 1.51	13.72	- 8.83	109.27	9.54 \pm 0.80	8.97	4.78	95.87
	20	18.05 \pm 0.79	4.53	- 2.39	87.04	14.87 \pm 3.52	11.98	12.50	76.98
	30	25.85 \pm 1.48	6.05	14.35	86.85	27.17 \pm 2.01	7.13	11.37	87.59
Sample 2	10	11.15 \pm 1.22	2.36	- 2.47	101.98	11.35 \pm 0.24	2.48	3.58	113.50
	20	18.98 \pm 0.0025	1.45	6.34	96.12	18.69 \pm 0.37	6.41	2.54	93.30
	30	30.08 \pm 0.04	2.45	8.27	98.09	27.05 \pm 4.77	13.69	8.02	89.80
Sample 3	10	7.50 \pm 0.39	6.81	15.03	73.65	8.31 \pm 0.24	3.52	14.65	83.12
	20	22.25 \pm 3.46	6.04	- 14.27	107.45	27.14 \pm 7.50	12.74	- 10.23	87.60
	30	30.50 \pm 3.47	12.04	- 1.63	102.12	39.56 \pm 3.22	9.51	- 10.87	113.04

The data are the mean \pm standard deviation from three studies. The correctness of an analytical procedure denotes the proximity between the anticipated value and the obtained value. The percent recovery (%) of the analyte recovered is calculated.

The raw sample of Verapamil HCl exhibited pronounced and extensive peaks at wavelengths of 2990.02 cm^{-1} , 2955.68 cm^{-1} , 2937.08 cm^{-1} , and 2905.61 cm^{-1} , suggesting the presence of the C-H group (Figure 06) (Daud et al., 2021). Ultimately, the analysis of Verapamil HCL with Sample 1 was conducted at various ratios (1:3, 1:5, 1:7, 1:9), yielding spectral readings of 3443.52 cm^{-1} , 3432.08 cm^{-1} , 3462.12 cm^{-1} , and 3443.52 cm^{-1} , which indicate the presence of N-H and O-H bonds produced by sp^3 hybridization (Figure 2-4).

3.3 Method Development

Diverse chromatographic techniques have been established to quantify VPM, Sample 1, Sample 2, and Sample 3 in particular formulations, often with additional compounds (Poukarim et al., 2019). Numerous procedures need extended analytic durations, rendering them inappropriate for routine evaluation. Moreover, there is yet no technique for concurrently identifying the research participant using HPLC detection in biological fluids. Therefore, there is an urgent need to devise a more pragmatic approach that offers more easy alternatives with satisfactory detection and quantification thresholds. Consequently, we devised and validated an RP-HPLC technique for their measurement in plasma. The parameters necessary for achieving high sensitivity and selectivity were optimized.

Comment [AS6]: •Clarify the relevance of the observed changes (specific interaction, structural modification) in peak positions.
•Why some peaks are missing?

3.4 Optimization of Separation Conditions

Various reversed-phase columns and gradient mobile phases were examined to identify the optimal conditions for chromatographic separation of the target analytes using a simultaneous approach. Table 1 presents the analytical parameters for the robustness of the HPLC approach in the concurrent measurement of VPM and CAs. VPM and CA are hydrophilic; hence, C18 reversed-phase columns were used to provide optimal run duration, symmetrical peak shape, and enhanced resolution. The superior resolution of these pharmaceuticals was attained using the Phenomenex C18 (4.6 × 150 mm, 5 μm) column, which is extensively used for the separation of VPM and CA. Initially, isocratic elution was used for the separation of the analytes. Nevertheless, it was unable to concurrently separate the target analytes; so, gradient elution was used for optimal separation and adequate resolution. The separation of VPM, Samples 1, 2, and 3 was conducted on a Phenomenex C18 column (150 × 4.6 mm) with a 5 μm particle size (Shimadzu, UV detector 20A, Kyoto, Japan), using HPLC grade water as mobile phase A and acetonitrile as mobile phase B in a linear gradient elution mode (A:B). The flow rate was established at 0.5 mL/min, and the column temperature was maintained at 35 °C. The simultaneous analysis of the VPM, 1, 2, and 3 samples was conducted using the internal standard technique at a wavelength of 280 nm. The internal standard was analyzed at a wavelength of 280 nm under identical conditions.

3.5 Method Validation

The existing methodology was validated in accordance with the U.S. Guidance for Industry on Bioanalytical Method Validation and the criteria specified in the Experimental Procedures section (Moein et al., 2017). A simple linear equation generated a linear correlation under optimal experimental conditions. The calibration curve was constructed using peak area in relation to concentration. The assessment of the negative control sample examined this procedure; the negative control sample was spiked with the analytes, and control samples were taken at 0.5, 1, 2, 3, 5, and 6 hours post-administration of the combination. Representative chromatograms of these samples are shown in Figure 4. The identification of VPM, Sample 1, Sample 2, and Sample 3 using HPLC with a UV detector shown good selectivity, devoid of interference from one another and endogenous compounds. The retention times for VPM, Sample 1, Sample 2, and Sample 3 were 6.5 ± 0.2 , 2.6 ± 0.1 , and 5.3 ± 0.2 , respectively, within a runtime of 20.00 minutes. All calibration curves exhibited strong linearity within the specified ranges, with correlation coefficient (r) values above 0.94. The limits of detection (LOD) and quantitation (LOQ) were established by injecting diluted reference solutions onto the HPLC column under optimized chromatographic conditions (Table 3) (Haddad et al., 2020). The limit of detection (LOD) values were 0.4 ng/mL for VPM, 0.55 ng/mL for Sample 1, 15.14 ng/mL for Sample 2, and 0.05 ng/mL for Sample 3, respectively. The LOQ values were 1.53, 1.73, 69.24, and 0.11 ng/mL for VPM, Sample 1, Sample 2, and Sample 3, respectively. All analytes evaluated with the assay, peak eight, theoretical plates, tailing factor, and capacity factors fell within the acceptable

Comment [AS7]: More discussion could be added regarding the implications of the LOD and LOQ values, especially in relation to the sensitivity of the method.

range. The test result was determined to be within the 90–115% range, which is deemed adequate according to the FDA Guidance for Industry on Bioanalytical Method Validation (Şengül et al., 2016). The tailing factor and capacity factor for VPM, Sample 1, Sample 2, and Sample 3 were 0.77, 1.43, 0.83, and 1.82, 2.6, 0.71, 1.48, and 0.75, respectively. The findings confirmed the lack of interferences in the samples and the absence of peaks in the negative control related to any of the analyzed analytes.

Comment [AS8]: Ensure that all cited references are properly formatted according to the chosen citation style.

3.6 Precision, Accuracy, Recovery and Robustness

The precision, accuracy, recovery, and absolute matrix impact of this method were assessed (Table 4). The intra- and inter-assay bias precision and accuracy were quantified as standard deviation (SD) and relative error (RE), respectively, not surpassing $\pm 15\%$. The determined recoveries and absolute matrix effect values ranged from 85.0% to 115% (Bonfilio et al., 2012).

All findings demonstrated that the test was both repeatable and accurate for quantifying VPM, Sample 1, Sample 2, and Sample 3. Table 3 presents flow rates of 0.3 mL/min and 0.5 mL/min, with consistent chromatographic conditions, including a wavelength of 280 nm, a column size of 150 × 4.6 mm, and a column temperature of 35 °C (Fekete et al., 2014). Acetonitrile and methanol were used separately in gradient elution; however, optimal sample separation was achieved with acetonitrile. Sample separation was not accomplished using methanol owing to its polar characteristics. Furthermore, acetonitrile has a lower UV cut-off than methanol, making it more appropriate for applications necessitating low UV detection wavelengths. Moreover, acetonitrile/water mixtures exhibit lower viscosity than methanol/water mixtures, resulting in significantly reduced back pressures throughout the column (Desai et al., 2011). The reduced pressure in the lower back is often seen as beneficial, since it lowers stress on the system components and column, allowing for an increase in flow rate and a decrease in operational durations. When acetonitrile and methanol are combined with water in same proportions, the acetonitrile mobile phase exhibits superior elution strength. Under chromatographic circumstances, the oven temperature was seen to remain stable between 30–35 °C, showing no significant variation.

Comment [AS9]: •Clarity of sentence structure is needed for readability and flow.
•Consistent use of terminology and formatting across the manuscript.
•Justifications for the choice of acetonitrile over methanol are well-explained with supporting references.
• Please provide the technical details on the method robustness.

4. CONCLUSION

This research examined the interactions between Verapamil HCl and citric acid utilizing FT-IR, HPLC, and UV-Vis spectroscopy, with an emphasis on different drug-to-excipient ratios (1:3, 1:5, and 1:7). The findings indicated that the interactions were primarily physical, with no notable chemical changes detected, as confirmed by consistent spectral profiles and the lack of new functional group formations. Citric acid enhanced the solubility and bioavailability of Verapamil HCl while maintaining its structural integrity and therapeutic efficacy. The results highlight the promise of citric acid as a reliable and secure excipient in pharmaceutical formulations, especially for enhancing the effectiveness of poorly water-soluble medications. Furthermore, this study underscores the significance of systematic analytical methodologies in ensuring drug stability and

establishes a basis for future investigations into excipient-API interactions across various conditions.

Comment [AS10]: • Integration of result data relate to the enhancement of Verapamil HCl's therapeutic efficacy more explicitly.
•grammatical improvements.

REFERENCE

Alquadeib, B. T. (2019). Development and validation of a new HPLC analytical method for the determination of diclofenac in tablets. *Saudi pharmaceutical journal*, 27(1), 66-70. <https://doi.org/10.1016/j.jsps.2018.07.020>

Bezzon, V. D., Ferreira, F. F., & de Lima, J. C. (2021). Local atomic structure determination of the amorphous verapamil HCl drug. *Journal of Non-Crystalline Solids*, 565, 120856. <https://doi.org/10.1016/j.jnoncrysol.2021.120856>

Bialer, M., & Soares-da-Silva, P. (2012). Pharmacokinetics and drug interactions of eslicarbazepine acetate. *Epilepsia*, 53(6), 935-946. <https://doi.org/10.1111/j.1528-1167.2012.03519.x>

Bonfilio, R., Cazedey, E. C. L., Araújo, M. B. D., & Nunes Salgado, H. R. (2012). Analytical validation of quantitative high-performance liquid chromatographic methods in pharmaceutical analysis: a practical approach. *Critical Reviews in Analytical Chemistry*, 42(1), 87-100. <https://doi.org/10.1080/10408347.2012.630926>

Bulduk, İ. (2021). Comparison of HPLC and UV spectrophotometric methods for quantification of favipiravir in pharmaceutical formulations. *Iranian journal of pharmaceutical research: IJPR*, 20(3), 57. <https://doi.org/10.22037/ijpr.2020.114199.14725>

Cinar, M., Can, S., Baris, Ö, & Demirci, Ç. E. (2024). Diltiazem and Verapamil: Combined experimental and computational approaches to structural and spectroscopic characterization. *Journal of Molecular Structure*, 1295, 136712. <https://doi.org/10.1016/j.molstruc.2023.136712>

Daud, H., Ghani, A., Iqbal, D. N., Ahmad, N., Nazir, S., Muhammad, M. J., & Iqbal, M. (2021). Preparation and characterization of guar gum based biopolymeric hydrogels for controlled release of antihypertensive drug. *Arabian Journal of Chemistry*, 14(5), 103111. <https://doi.org/10.1016/j.arabjc.2021.103111>

Desai, A. M., Andreae, M., Mullen, D. G., Holl, M. M. B., & Baker Jr, J. R. (2011). Acetonitrile shortage: Use of isopropanol as an alternative elution system for ultra/high

performance liquid chromatography. *Analytical Methods*, 3(1), 56-58. <https://doi.org/10.1039/C0AY00493F>

Faghihzadeh, F., Anaya, N. M., Schifman, L. A., & Oyanedel-Craver, V. (2016). Fourier transform infrared spectroscopy to assess molecular-level changes in microorganisms exposed to nanoparticles. *Nanotechnology for Environmental Engineering*, 1, 1-16. <https://doi.org/10.1007/s41204-016-0001-8>

Fekete, S., Kohler, I., Rudaz, S., & Guillarme, D. (2014). Importance of instrumentation for fast liquid chromatography in pharmaceutical analysis. *Journal of pharmaceutical and biomedical analysis*, 87, 105-119. <https://doi.org/10.1016/j.jpba.2013.03.012>

Fung, M. H., DeVault, M., Kuwata, K. T., & Suryanarayanan, R. (2018). Drug-excipient interactions: effect on molecular mobility and physical stability of ketoconazole–organic acid coamorphous systems. *Molecular pharmaceutics*, 15(3), 1052-1061. <https://doi.org/10.1021/acs.molpharmaceut.7b00932>

Ghorpade, V. S., Yadav, A. V., & Dias, R. J. (2017). Citric acid crosslinked β -cyclodextrin/carboxymethylcellulose hydrogel films for controlled delivery of poorly soluble drugs. *Carbohydrate Polymers*, 164, 339-348. <https://doi.org/10.1016/j.carbpol.2017.02.005>

Gorain, B., Choudhury, H., Pandey, M., Madheswaran, T., Kesharwani, P., & Tekade, R. K. (2018). Drug–excipient interaction and incompatibilities. In *Dosage form design parameters* (pp. 363-402). Academic Press. <https://doi.org/10.1016/B978-0-12-814421-3.00011-7>

Govindarajan, R., Landis, M., Hancock, B., Gatlin, L. A., Suryanarayanan, R., & Shalae, E. Y. (2015). Surface acidity and solid-state compatibility of excipients with an acid-sensitive API: case study of atorvastatin calcium. *AAPS PharmSciTech*, 16, 354-363. <https://doi.org/10.1208/s12249-014-0231-7>

Haddad, P. R., Taraji, M., & Szücs, R. (2020). Prediction of analyte retention time in liquid chromatography. *Analytical Chemistry*, 93(1), 228-256. <https://doi.org/10.1021/acs.analchem.0c04190>

Lambros, M., Tran, T., Fei, Q., & Nicolaou, M. (2022). Citric acid: A multifunctional pharmaceutical excipient. *Pharmaceutics*, 14(5), 972. <https://doi.org/10.3390/pharmaceutics14050972>

Li, Y., Zhang, D., Ash, J., Jia, X., Leone, A., & Templeton, A. (2019). Mechanism and impact of excipient incompatibility: Cross-linking of xanthan gum in pediatric powder-for-suspension formulations. *Journal of Pharmaceutical Sciences*, 108(11), 3609-3615. <https://doi.org/10.1016/j.xphs.2019.07.005>

Moein, M. M., El Beqqali, A., & Abdel-Rehim, M. (2017). Bioanalytical method development and validation: Critical concepts and strategies. *Journal of Chromatography B*, 1043, 3-11. <https://doi.org/10.1016/j.jchromb.2016.09.028>

Nadimi, A. E., Ebrahimipour, S. Y., Afshar, E. G., Falahati-Pour, S. K., Ahmadi, Z., Mohammadinejad, R., & Mohamadi, M. (2018). Nano-scale drug delivery systems for antiarrhythmic agents. *European journal of medicinal chemistry*, 157, 1153-1163. <https://doi.org/10.1016/j.ejmech.2018.08.080>

Nangare, S., Vispute, Y., Tade, R., Dugam, S., & Patil, P. (2021). Pharmaceutical applications of citric acid. *Future Journal of Pharmaceutical Sciences*, 7, 1-23. <https://doi.org/10.1186/s43094-021-00203-9>

Pourkarim, F., Rahimpour, E., & Jouyban, A. (2019). Analytical techniques for the determination of verapamil in biological samples and dosage forms: an overview. *Bioanalysis*, 11(23), 2189-2205. <https://doi.org/10.4155/bio-2019-0083>

Sahu, P. K., Ramiseti, N. R., Cecchi, T., Swain, S., Patro, C. S., & Panda, J. (2018). An overview of experimental designs in HPLC method development and validation. *Journal of pharmaceutical and biomedical analysis*, 147, 590-611. <https://doi.org/10.1016/j.jpba.2017.05.006>

Sanam, S., Halder, S., & Rahman, S. A. (2023). Simultaneous Pharmacokinetic Evaluation of Pantoprazole and Vitamin B Complex for Assessing Drug-Drug Interactions in Healthy Bangladeshi Adults by a Newly Developed and Validated HPLC Method. *Separations*, 10(3), 170. <https://doi.org/10.3390/separations10030170>

Şengül, Ü. (2016). Comparing determination methods of detection and quantification limits for aflatoxin analysis in hazelnut. *Journal of Food and Drug Analysis*, 24(1), 56-62. <https://doi.org/10.1016/j.jfda.2015.04.009>

Shinkar, D. M., Aher, P. S., Kothawade, P. D., & Maru, A. D. (2018). Formulation and in vitro evaluation of fast dissolving tablet of verapamil hydrochloride. *Int J Pharm Pharm Sci*, 10(10), 93-9. <http://dx.doi.org/10.22159/ijpps.2018v10i10.28714>

Shomudro, H. K., Khatun, T., & Sanam, S. (2022). A validated RP-HPLC method for analysis of chloramphenicol residue in pasteurized milk sample in Bangladesh. *International Journal of Scientific and Engineering Research*, 7(9), 33-40.

Srinivasan, V., Sivaramakrishnan, H., & Karthikeyan, B. (2011). Detection, isolation and characterization of principal synthetic route indicative impurities in verapamil hydrochloride. *Scientia Pharmaceutica*, 79(3), 555. <https://doi.org/10.3797/scipharm.1101-19>

Studzińska-Sroka, E., Dudek-Makuch, M., Chanaj-Kaczmarek, J., Czepulis, N., Korybalska, K., Rutkowski, R. & Witowski, J. (2018). Anti-inflammatory Activity and Phytochemical Profile of *Galinsoga Parviflora* Cav. *Molecules*, 23(9), 2133. <https://doi.org/10.3390/molecules23092133>

Wen, H., Jung, H., & Li, X. (2015). Drug delivery approaches in addressing clinical pharmacology-related issues: opportunities and challenges. *The AAPS journal*, 17, 1327-1340. <https://doi.org/10.1208/s12248-015-9814-9>

Yin, H., & Zhu, J. (2023). Methods for quantification of glycopeptides by liquid separation and mass spectrometry. *Mass spectrometry reviews*, 42(2), 887-917. <https://doi.org/10.1002/mas.21771>

Zhou, P., Zhang, S. M., Wang, Q. L., Wu, Q., Chen, M., & Pei, J. M. (2013). Anti-arrhythmic effect of verapamil is accompanied by preservation of cx43 protein in rat heart. *PLoS One*, 8(8), e71567. <https://doi.org/10.1371/journal.pone.0071567>

Comment [AS11]:

Comment [AS12]: •Ensure that all references have complete information.
•In some references, page numbers are not explicitly mentioned.

UNDER PEER REVIEW